

Hall Effect through Magnetic Phase Transitions in Nd₂Fe₁₄B

Jolanta Stankiewicz* and Juan Bartolomé

*Instituto de Ciencia de Materiales de Aragón, Consejo Superior de Investigaciones Científicas,
and Universidad de Zaragoza, 50009-Zaragoza, Spain*

(Received 17 May 1999)

We have observed large variations of the Hall effect in the vicinity of magnetic phase transition points. Sharp peaks near the spin-reorientation and Curie temperatures are observed in Hall effect data from Nd₂Fe₁₄B single crystals. The effect is very sensitive to the applied magnetic field direction near the spin-reorientation temperature. Away from these critical regions the Hall resistivity is proportional to the square of the total resistivity. Different scattering mechanisms dominate in different regions.

PACS numbers: 72.15.Gd, 75.50.Bb

The electrical resistivity of metallic ferromagnets and antiferromagnets exhibits some anomalies at the critical points. Critical magnetic fluctuations underlie these anomalies [1,2]. The Hall effect exhibits in magnetic materials some unusual features as well. The anomalous Hall resistivity is known to increase with temperature in the ferromagnetic phase, up to a maximum value, close to the Curie temperature, and drops rapidly thereafter to low values in magnetic metals such as nickel or iron [3]. The Hall resistivity shows a rather complex behavior in rare-earth single crystals [4]. Existing theories do not account satisfactorily for the observed behavior even though good agreement can sometimes be obtained over a limited temperature range [5].

The spontaneous (or anomalous) Hall effect (SHE) arises from asymmetric (with respect to a plane defined by the carrier's incoming direction and its spin direction) scattering of the current carriers which are subject to spin-orbit interactions. In itinerant magnetism models, intrinsic spin-orbit interaction of polarized electrons produces a steady Hall current. Karplus and Luttinger obtained $\rho_H \propto \rho^2 \langle M \rangle$, where ρ_H is the Hall resistivity, ρ is the total resistivity, and M is the system magnetization [6]. This theory has, however, been criticized, and the relation $\rho_H \propto \rho \langle M \rangle$ has been proposed [7]. Ions with localized d (f) electrons can also produce classical skew scattering of conduction s electrons if intrinsic spin-orbit interaction of d electrons within magnetic ions or extrinsic d spin- s orbit interaction is taken into account [8,9]. In the theories with localized spins, $\rho_H \propto M_3$, where $M_3 = \langle (M_H - \langle M_H \rangle)^3 \rangle$, and M_H is the magnetization along the magnetic field direction. In addition to skew scattering, a nonclassical effect of a lateral displacement Δy (side jump) of the charge carrier's trajectory at every scattering event, either by impurities or by phonons, can be important in the SHE of concentrated alloys [10]. This mechanism, if there are spin-orbit interactions, gives $\rho_H \propto \rho^2 \langle M \rangle$. Surprisingly, most of these theories seem to account for the data from Ni and Fe in spite of the different underlying mechanisms. The importance of the various mechanisms responsible for the anomalies of

the Hall effect in magnetic systems has not yet been clearly established.

The anomalous Hall resistivity can be a sensitive probe of the interplay between electronic and magnetic phenomena. However, not many experiments have been reported on this subject [5]. It is our aim to study the Hall effect through different magnetic phase transitions and thus to pinpoint the role that different scattering mechanisms play in bringing about the anomalous Hall effect. Large variations of the Hall effect can be expected near critical points. This happens in Nd₂Fe₁₄B which is an important magnetic material for technological applications as a permanent magnet.

The compound Nd₂Fe₁₄B crystallizes in a tetragonal structure. Its magnetic properties are well known [11]. The Fe sublattice gives most of the magnetization of Nd₂Fe₁₄B while the magnetocrystalline anisotropy arises almost entirely from the Nd ions. The Nd and Fe sublattice moments couple ferromagnetically; the Curie temperature, T_c , is 586 K [12]. Below T_c , the easy magnetization direction is the tetragonal c axis and the Nd and Fe sublattice moments are collinear. At lower temperatures, Nd₂Fe₁₄B exhibits a continuous spin-reorientation transition. Below the spin-reorientation temperature, T_s ($T_s \approx 130$ K), the magnetization direction cants away from the [001] towards the [110] direction, by an angle that increases with decreasing temperature, up to approximately 30° at 4 K. Thus, electronic transport properties in the vicinity of two critical points can be studied in this system.

In this Letter we report results of Hall effect measurements in a single crystal of Nd₂Fe₁₄B for a wide temperature range (4–700 K) and various magnetic field orientations with respect to the easy-magnetization axis. Large variations of the Hall resistivity are observed in the vicinity of both the paramagnetic-ferromagnetic and the spin-reorientation transitions. The temperature dependence of the anomalous Hall coefficient in the magnetic phase transition regions follows the third moment of the magnetization fluctuations. Away from these regions, the anomalous Hall coefficient is proportional to the square

of total resistivity, as predicted for side-jump scattering in magnetic materials.

The electrical resistivity and Hall effect measurements were performed with a six probe method on bar shaped samples. The typical dimensions of the samples were of $0.7 \times 1 \times 5 \text{ mm}^3$. X-ray diffraction was used to orient the crystal. The Hall resistivity was measured as a function of magnetic field up to 0.6 T. Magnetization measurements were performed with a SQUID magnetometer for temperatures below 400 K, and with a Faraday balance for higher temperatures on the same samples that were used in magnetotransport studies.

How the zero-field resistivity and the low-field (0.1 T) Hall resistivity of $\text{Nd}_2\text{Fe}_{14}\text{B}$ single crystals vary with temperature in the range from 4 to 700 K is shown in Fig. 1. The current flow was always perpendicular to the c axis. The resistivity varies smoothly with temperature, except for a small dip near T_c . Its behavior has been discussed in our earlier papers [13]. We note that our samples have a rather high value of the residual resistivity ($\rho_o \cong 35 \mu\Omega \text{ cm}$), which shows that there are large impurity concentrations and/or static lattice imperfections. On the other hand, the Hall resistivity of $\text{Nd}_2\text{Fe}_{14}\text{B}$, which is holelike, varies strongly with temperature. For \mathbf{H} perpendicular to the c axis, it passes through a sharp maximum near 130 K and a slight one near 580 K. For the parallel configuration, ρ_H increases as T increases up to T_c , where it drops sharply to very low values. It shows no anomaly close to T_s , in contrast with the behavior exhibited in the $\mathbf{H} \perp [001]$ case.

Phenomenologically, the Hall resistivity is given by $\rho_H = R_o B + R_s 4\pi M$, where R_o is the ordinary Hall coefficient, R_s is the SHE coefficient, B is the applied magnetic induction, and M is the spontaneous magnetization. In our samples, the R_s is much larger than R_o ($R_o \leq 0.01 R_s$) [13]. Therefore, we obtain the values of the SHE coefficient from $R_s = \rho_H / 4\pi M$, where ρ_H is the low-field Hall resistivity (shown in Fig. 1) and M is the value of magnetization measured with the same field

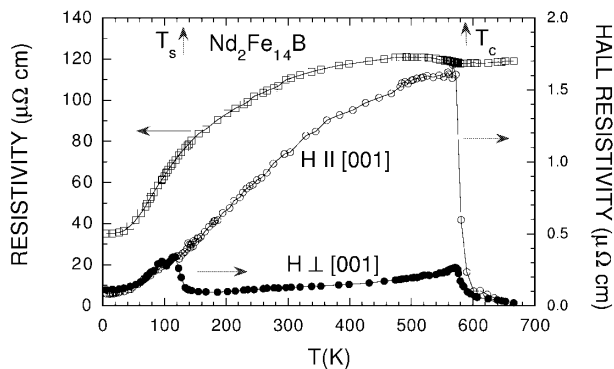


FIG. 1. Zero-field resistivity and low-field (0.1 T) Hall resistivity data points versus temperature of $\text{Nd}_2\text{Fe}_{14}\text{B}$ single crystals. The solid lines are guides to the eye.

(0.1 T) applied to the same sample. Since the anisotropy field of $\text{Nd}_2\text{Fe}_{14}\text{B}$ is high (7.3 T at 300 K), the field we applied, 0.1 T, is too small to saturate magnetization even in the easy direction. Consequently, we are in the linear part of the $M(B)$ and $\rho_H(B)$ curves, which are sample shape dependent. In addition, magnetic domains in the material studied change at the spin reorientation transition [14]. However, by relating the values of ρ_H and M measured on the same sample to the same field we expect to avoid shape and domain related effects.

The temperature variations of R_s and of M are shown in Fig. 2. For $\mathbf{H} \perp [001]$, the magnetization rises sharply upon cooling, near the spin-reorientation temperature. The rise might seem overly steep, but this is so only because domains in the system restrict the rise of $M(T)$ beyond 200 G, which is only 0.15 of its saturation value. Thus, the upper part of the magnetization curve, above 200 G, where it gradually bends over [12], is missing in Fig. 2. A trace of the spin-reorientation transition is also clearly seen in the anomalous Hall coefficient as a dip near T_s . There is some small feature in R_s near T_c for this configuration. In contrast, for $\mathbf{H} \parallel [001]$, R_s shows a sharp minimum at T_c . Away from the magnetic critical regions, $R_s \propto \rho^2$ for both configurations. Such behavior of the SHE coefficient is in agreement with (a) near

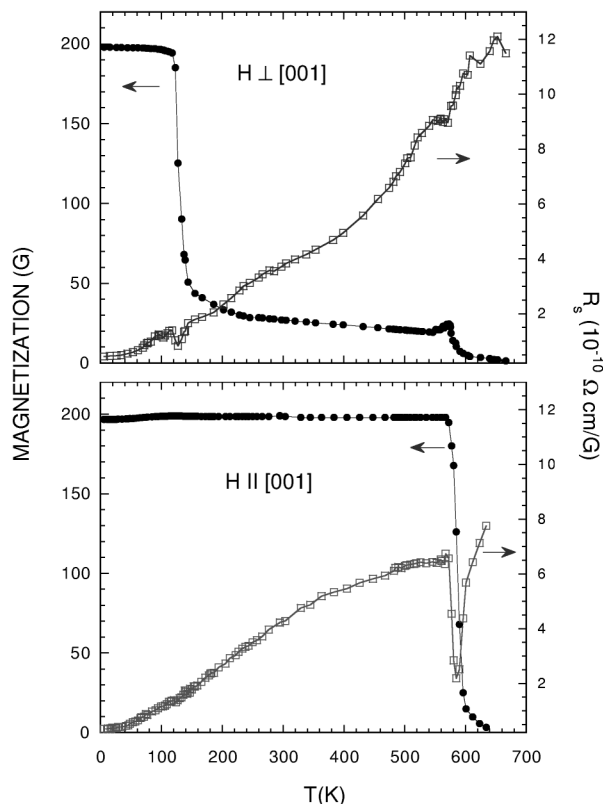


FIG. 2. Magnetization at $H = 0.1 \text{ T}$ and the anomalous Hall coefficient as a function of temperature for $\text{Nd}_2\text{Fe}_{14}\text{B}$ single crystal at two different magnetic field directions. The solid lines are guides to the eye.

critical points the dominant asymmetric scattering comes from magnetization fluctuations and (b) away from critical points, ρ_H is limited by side-jump scattering as it occurs in materials with large ρ . The first point is clear from the configurational dependence of R_s : critical magnetization fluctuations are expected in the plane perpendicular to the c easy axis since Fe and Nd magnetic moments cant away from it below $T \cong T_s$. It follows therefore from $\rho_H \propto M_3$ [9] that the variations in R_s can be also large. However, magnetization fluctuations are expected to be small along the [001] easy direction. On the other hand, in the vicinity of T_c , the longitudinal magnetic fluctuations are critical, whereas transversal ones are not so. This is clearly observed in our experiment.

Following theoretical predictions [8–10], we fit the experimental results to the relation $R_s = aM_3/4\pi M + b\rho^2$, where the first and second terms give the skew component and the side-jump contributions, respectively, to the SHE. We have calculated the third moment of the magnetization fluctuations, M_3 , within a phenomenological molecular-field model for an anisotropic ferromagnet [15,16]. In this model, the anisotropy energy is of the form $E_{\text{an}}^R = K_1 \sin^2\theta + \tilde{K}_2 \sin^4\theta + \tilde{K}_3 \sin^6\theta$ and $E_{\text{an}}^{\text{Fe}} = K_0 \sin^2\theta$ for the rare-earth and Fe ion, respectively [16,17]. Here, K_1 , \tilde{K}_2 , \tilde{K}_3 , and K_0 are temperature-dependent uniaxial-anisotropy constants, and θ is the angle between the c axis and the magnetization vector. We assume that the Nd (μ_R) and Fe (μ_{Fe}) moments are collinear and that the Nd-Nd exchange is negligible [11]. The total magnetic energy of $\text{Nd}_2\text{Fe}_{14}\text{B}$ per unit cell can be written

$$E = 4E_{\text{an}}^R + 28E_{\text{an}}^{\text{Fe}} - (4\mu_R + 28\mu_{\text{Fe}})H \cos(\theta - \delta) - 56n_{\text{RF}}\mu_R\mu_{\text{Fe}} - 14n_{\text{FF}}\mu_{\text{Fe}}\mu_{\text{Fe}}, \quad (1)$$

where molecular-field coefficients (dimensionless) n_{RF} and n_{FF} describe the R-Fe and Fe-Fe magnetic interaction, respectively, and δ is the angle between the external magnetic field and the c axis. We assume that a Brillouin function with a molecular field for each component governs the temperature dependence of μ_R and μ_{Fe} [11]. $M(H, T)$ follows from the equilibrium condition $dE/d\theta = 0$. The spin-moment fluctuations have been obtained by taking the second derivative (numerically) of the magnetization with respect to the magnetic field, making use of the basic relation $\langle(M_H - \langle M_H \rangle)^3\rangle = (k_B T)^2 (\partial^2 M_H / \partial H^2)_T$ (k_B is the Boltzmann constant). Values of $K_0(T)$, $K_1(T)$, $\tilde{K}_2(T)$, and $\tilde{K}_3(T)$ were taken from Refs. [12] and [15,17]. A slight change (within 5%) in the value of K_1 leads to a significant improvement of our fits. We use the “corrected” anisotropy constant values throughout this paper. We found that values of 5.8×10^3 for n_{FF} and of 2×10^3 for n_{RF} give the best fit between the calculated and the measured magnetization at saturating field [12]. These values differ less than 10% from the reported ones [11]. The free-ion moment was used as the zero-temperature moment of Nd ions. We

assume a value of $2\mu_B$ for $\mu_{\text{Fe}}(0)$ and a value of 1 for the Fe spin (μ_B in the Bohr magneton) [12].

The best fit to the spontaneous Hall coefficient, shown in Fig. 3 by the solid line, yields $b = 0.03 \Omega^{-1} \text{cm}^{-1} \text{G}^{-1}$ for both configurations and $a = 1 \times 10^{25} (0.5 \times 10^{24}) \Omega \text{cm}^{-5} \text{G}^{-3}$ for \mathbf{H} perpendicular (parallel) to the c axis. These values are not far from theoretically predicted values [9,10]. Our calculations reproduce very well the observed experimental features: a pronounced negative peak in $\partial^2 M_H / \partial H^2$ slightly below T_s for $\mathbf{H} \perp [001]$ and at T_c for $\mathbf{H} \parallel [001]$. We did not extend our calculations beyond T_c since the values of the system constants are not known therein.

In conclusion, we show that a combination of skew and side-jump scattering explains our experimental results for SHE in $\text{Nd}_2\text{Fe}_{14}\text{B}$ in the whole temperature range studied. Skew scattering by spin fluctuations is only dominant in a narrow temperature region near the critical points. Our results show the importance of localized spin - charge carrier interaction therein. Away from critical regions, SHE appears to be caused by side-jump scattering. The length of the side jump, obtained from the Hall angle variation with magnetization, amounts to $2 \times 10^{-9} \text{cm}$, which is very close to the one-band estimate in ferromagnetic materials [10].

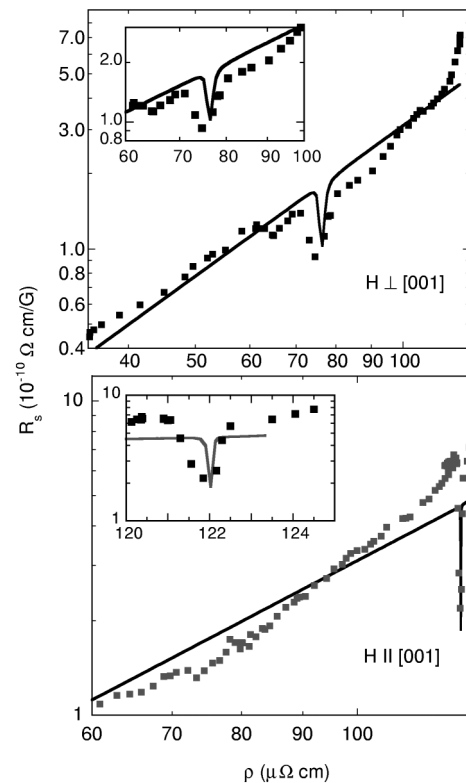


FIG. 3. Anomalous Hall coefficient as a function of the total resistivity for $\text{Nd}_2\text{Fe}_{14}\text{B}$ single crystal. The solid lines are fits to experimental points. The inset shows the spin reorientation (upper panel) and the paramagnetic-ferromagnetic phase transition region (lower panel) in detail.

We find experimentally that the low-field Hall resistivity passes through a pronounced maximum in the vicinity of the spin-reorientation temperature and changes abruptly at the Curie temperature in $\text{Nd}_2\text{Fe}_{14}\text{B}$. These are the largest electronic transport effects we know of that can be attributed to magnetic phase transitions. We should note that the electrical conductivity does not show anomalies at the critical points except for a small dip near T_c . This is as expected since magnetization fluctuations affect conductivity much less than the SHE. The magnetic resistivity is proportional to the second moment of the magnetization which has a weaker critical divergence than M_3 does [18]. In addition, scattering mechanisms that are magnetization independent, such as scattering by impurities or static lattice defects, mask magnetization-dependent effects in the total resistivity.

The single crystal of $\text{Nd}_2\text{Fe}_{14}\text{B}$ used in our study has been grown by Dr. S. Hirosawa of Sumitomo Special Metals. This work was supported by Project MAT 96-448 of Comisión Interministerial de Ciencia y Tecnología (CICYT).

*Email address: jolanta@posta.unizar.es

- [1] P.G. de Gennes and J. Friedel, *J. Phys. Chem. Solids* **4**, 71 (1958).
- [2] M.E. Fisher and J.S. Langer, *Phys. Rev. Lett.* **20**, 665 (1968).
- [3] J.-P. Jan, *Helv. Phys. Acta* **25**, 677 (1952); J.-P. Jan and J.M. Gijnsman, *Physica (Utrecht)* **18**, 339 (1952).
- [4] J.J. Rhyne, *Phys. Rev.* **172**, 523 (1968).
- [5] C.M. Hurd, in *The Hall Effect in Metals and Alloys* (Plenum Press, New York, London, 1972).
- [6] R. Karplus and J.M. Luttinger, *Phys. Rev.* **95**, 1154 (1954).
- [7] J. Smit, *Physica (Utrecht)* **21**, 877 (1955); **24**, 39 (1958).
- [8] J. Kondo, *Prog. Theor. Phys.* **27**, 772 (1962).
- [9] F.E. Maranzana, *Phys. Rev.* **160**, 421 (1967).
- [10] L. Berger, *Phys. Rev. B* **2**, 4559 (1970).
- [11] See J.F. Herbst, *Rev. Mod. Phys.* **63**, 819 (1991), and references therein.
- [12] S. Hirosawa, Y. Matsuura, H. Yamamoto, S. Fujimura, M. Sagawa, and H. Yamauchi, *J. Appl. Phys.* **59**, 873 (1986).
- [13] J. Stankiewicz and J. Bartolomé, *Phys. Rev. B* **55**, 3058 (1997); **59**, 1152 (1999).
- [14] Yu.G. Pastushenkov, A. Forkl, and H. Kronmüller, *J. Magn. Magn. Mater.* **174**, 278 (1997).
- [15] J.M. Cadogan, J.P. Gavigan, D. Givord, and H.S. Li, *J. Phys. F* **18**, 779 (1988).
- [16] M. Yamada, H. Kato, H. Yamamoto, and Y. Nakagawa, *Phys. Rev. B* **38**, 620 (1988).
- [17] F. Bolzoni, O. Moze, and L. Pareti, *J. Appl. Phys.* **62**, 615 (1987).
- [18] H.E. Stanley, *Introduction to Phase Transitions and Critical Phenomena* (Clarendon Press, Oxford, 1971), pp. 86–88.